A Comparison of Digital Transmission Techniques Under Multichannel Conditions at 2.4 GHz in the ISM BAND.

Fabien_Mulot (ONERA, TESA/SUPAERO, Fabien_Mulot@hotmail.com)
Vincent Calmettes (SUPAERO, vincent.calmette@supaero.fr)

ABSTRACT

In order to meet the observation quality criteria of the micro-UAVs, and particularly in the context of the « Trophée Micro-Drones », SUPAERO is studying technical solutions to transmit a high data rate from a video payload onboard a micro-UAV. The laboratory has to consider the impact of multipath and shadowing effects on the emitted signal (fig1.) and therefore it has to select fading resistant transmission techniques. The following of this paper discusses the study.

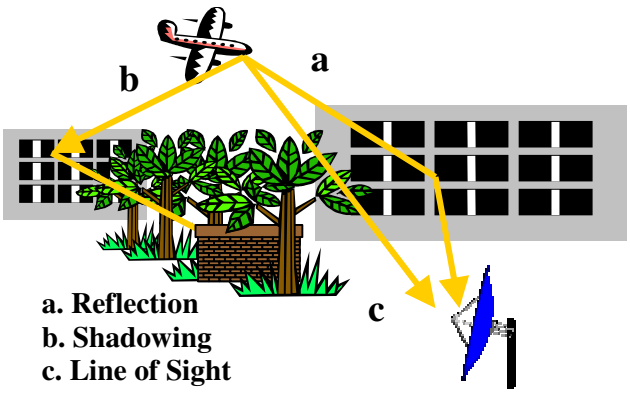

Figure 1. The wireless propagation landscape

1. INTRODUCTION

First, with the objective of achieving a video stream size around 1.5 Mbits·s^{-1} without coding, we defined a number of acceptable video characteristics in term of: refreshing rate, image resolution, and compression technique complexity.
Then the mobile propagation channel has been characterized.
We evaluated under Matlab/SIMULINK different transmission schemes (OFDM, Spread spectrum with rake receiver, QPSK with equalization) and different channel coding techniques (convolutional codes, Reed-Solomon codes).

The study had to reveal an optimum trade-off between three parameters, namely: the characteristics of the video stream, the complexity of the modulation and coding scheme, and the efficiency of the transmission, in term of BER.

2. CARACTERIZATION OF THE VIDEO STREAM

2.1 Description of the payload

The 640x480 pixels images are coded on 8 bits (256 grey levels). Then they are compressed in a JPEG format. See [Bur,03] for an example of a previously developed payload. JPEG is a lossy compression method because of the use of a quantification matrix. The losses are characterized by the creation of blocs on the image.

2.2 The different envisaged compression rates

The system will allow to switch between two modes. The first one, used for example in approach phases, will consist in a low resolution and a high image refreshing rate. The second one, used for more detailed scenes, will consist in a high resolution and a lower refreshing rate. Different compression rates have been selected (table1). A 10% extra margin has been added because the compression efficiency depends on the nature of the image. An image with large surfaces of the same color (low entropy) will give a smaller file size when compressed than an image with more colors (higher entropy) for the same quantification matrix.

Image	Compression Rate	Size [Ko]	+10% margin [Ko]
Uncompressed	1	302	-
A	33.5	9	10
B	20	15	16.5
C	10	28	31
D	8	38	42

Table 1. Image Size Vs Compression Rate

Image	Bit rate at 14 i/s	Bit rate at 2 i/s
A	1.12 Mbits/s	160 Kbits/s
B	1.848 Mbits/s	264 Kbits/s
C	3.472 Mbits/s	496 Kbits/s
D	4.704 Mbits/s	672 Kbits/s

Table 2. Bit rate Vs Image Rate

The table 2 shows different bit rates as a function of the number of images per second. These values will be used later in this paper.

The first picture below represents the uncompressed image. The pictures A to D correspond to the selected compression rates in tables 1 and 2. They show the impact of compression losses on the ability to read a text (Electronic) and to distinguish a face or a shape in a portion of the picture.

The 33.5% compression rate highly degrades the picture [A]. The face and the smallest inscription can't be distinguished. But the picture still contains enough details to allow the micro drone to navigate.

Unsurprisingly, the other compression rates give an increased quality but the data rates are bigger too. They can be used to provide more detailed scenes depending on the resolution required. But the counterpart will be a lower image refreshing rate.

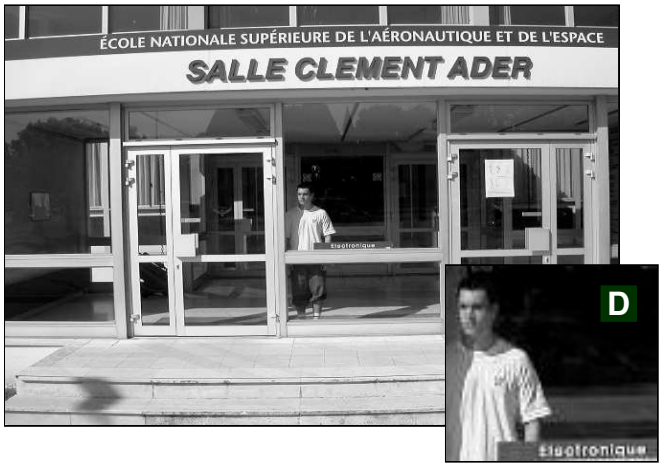

Picture 1. Visual effects of different compression rates

The strategy will be to provide a 1.12 Mbits/s video bit rate and therefore, either:

- 14 i/s in a low resolution [table1 A] or
- 3.3 i/s in a high resolution [table1 D].

3. MODELISATION OF THE WIRELESS CHANNEL

3.1 Transmission context

The band used for data transmission is the industrial, scientific, and medical ISM band. The usable bandwidth is around 79 MHz between 2.4 GHz and 2.485 GHz. This band is license free and standards using this band like Bluetooth and Wifi are open.
Concerning the emitted power, the maximum EIRP authorized by the ANFR (Agence Nationale des Frequences) is 10mW outdoor and 25 mW indoor.

3.2 General channel model

One subdivide the multiplicative fading processes in the channel into three types of fading: Path Loss, Shadowing and Multipath Fading. The Additive White Gaussian Noise is then taken into account.

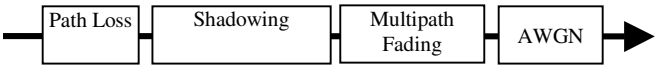

Figure 2. Wireless communication channel model

Path loss is given by $L=\left(\frac{\lambda}{4\pi d}\right)^2$ (Eq1)

d distance from the emitter to the receiver.

Shadowing changes more rapidly than path loss, with significant variations over distances of hundreds of meters and generally involving variations up to around 20 dB. The PDF of the attenuation process is log-normal; that is, the attenuation measured in decibel has a normal distribution.

Multipath fading involves faster variations of a scale of a half-wavelength (6.25 cm at 2.4 GHz) and generally introduces variations as large as 35 to 40 dB. It results from the constructive and destructive interference between multiple waves reaching the receiver.

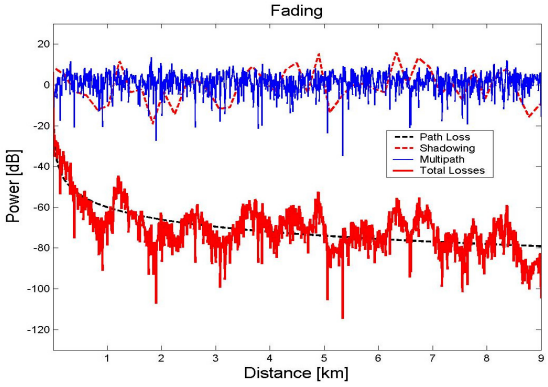

Figure 3. The three scales of mobile signal variation

3.2. Countering the Shadowing Effects

3.3. Multipath Channel Model

The figure 4 shows the standard form of the multipath channel model.

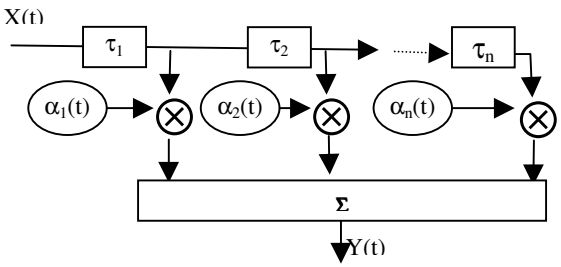

Figure 4. Standard Channel Model

The effects of scatterers in discrete delay ranges are lumped together into individual taps with the same delay. Each tap represents a single beam.

The gains α_n are varying in time independently of each other, according to the standard following laws: Rayleigh distribution, (Eq 2), for Non Line of Sight path and Rice distribution, (Eq 3), for LOS conditions. The worst case is the non LOS transmission where less power is available.

$$P_R(\alpha) = (\alpha/\sigma^2)e^{-(\alpha^2/(2\sigma^2))} \quad (2)$$

$$p_R(\alpha) = (\alpha/\sigma^2)e^{-(\alpha^2+s^2)/2\sigma^2} I_0(\alpha s/\sigma^2) \quad (3)$$

Table 3 gives a typical power-delay profile for mobiles communications. The first coefficient of the filter follows a Rice or a Rayleigh distribution for respectively a LOS or a non LOS transmission. In any cases, the other coefficients follow a Rayleigh law.

Tap	Delay µs	Average Power dB	Law	PSD
1	0.0	0	Rice or Rayleigh	Jakes
2	0.31	-5	Rayleigh	Jakes
3	0.71	-9	Rayleigh	Jakes
4	1.09	-11	Rayleigh	Jakes
5	1.73	-15	Rayleigh	Jakes
6	2.51	-20	Rayleigh	Jakes

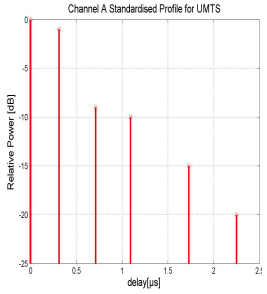

Table 3. Standard channel profile for UMTS

3.3.1. Second order fading statistics

In order to model the temporal autocorrelation of fades (depending on the speed of the mobile *v*), the following assumptions are made. The antenna of the receiver is omnidirectional. The arrival angle θ of waves is uniformly distributed around the receiver. Therefore, a suitable law is the classical Jakes' power density spectrum (Eq 4).

$$S(f)=\frac{E_0}{4\pi f_m}\frac{1}{\sqrt{1-(f/fm)^2}} \quad |f|<f_m \quad (4)$$

with $f = fc\frac{v}{c}\cos(\theta)$ (5)

- fm maximum Doppler shift
- Eo energy constant

3.3.2. Rice and Rayleigh fading models

The rician PDF is given by:

$$p_r(\alpha) = \frac{2k\alpha}{S^2} e(\frac{-k\alpha^2}{S^2}) e(-k) I_0(\frac{2k\alpha}{S}) \quad (6)$$

$$k = \frac{S^2}{2\sigma^2} = \frac{\mu^2}{2\sigma^2} \text{ and } E\left\{ r(t)^2 \right\} = P = 2\sigma^2 + \mu^2 \quad (7)$$

- S Magnitude of the LOS component
- σ^2 Variance of either the real or imaginary component.
- P average power given in table1

While μ=0 corresponds to the Rayleigh PDF, Rice and Rayleigh complex processes models are the following:

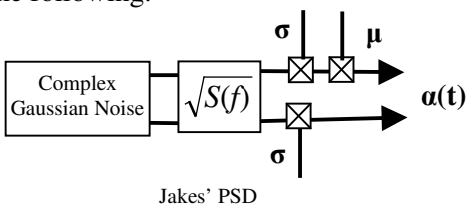

Figure 5.a Rice complex process

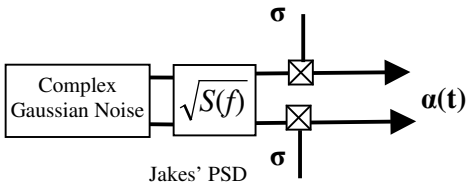

Figure 5.b Rayleigh complex process

The figure 6 shows the mobile channel model obtained using a 6 rays urban model for GSM

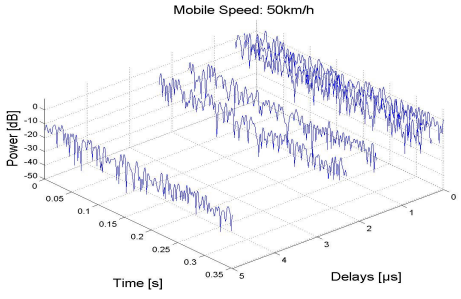

Figure 6. 6 rays urban model for GSM

3.3.3. Mobile radio channel characteristics at 2.4Ghz

a) Coherence time of the channel

When the response of a channel is time-variant, Doppler spread occurs. Signals which have less than Tc are received approximately undistorted by Doppler spread. [Saunders, 99] gives an approximation of the coherence time for the classical channel.

$$Tc = 9/(16\Pi fm) \quad (8)$$

The speed of the Micro UAV is in the range 0 - 50 km.h^{-1}. Eq (5) gives the corresponding Doppler fm ranging from 0 to 110Hz. Assuming a 110 Hz maximum Doppler , EQ (8) implicates Tc equal to 1.6 ms.

Therefore, signals with a rate lower than 625 Symb.s^{-1}will propagate in a fast varying channel; the channel varies during the propagation of the symbol and Doppler spread occurs. Signals with a higher rate will propagate in a slow varying channel without Doppler spread.

b) Coherence bandwidth

A closely related parameter to the coherence bandwidth Bc of the fading channel is the multipath spread Tm. Therefore the channel will be considered as non frequency selective if T>>Tm, where T is the symbol duration. In this case the channel is said to be flat in the frequency domain.

[Jakes,94] shows that assuming a classical Doppler spectrum for all components, the coherence bandwidth is:

$$Bc = \frac{\sqrt{3}}{22\Pi\tau_{rms}} \quad (9)$$

$$\tau_{rms} = \sqrt{\frac{1}{P_T}\sum_{i=1}^{n} P_i\tau_i^2 - \tau_0} \quad (10)$$

$$\tau_0 = \frac{1}{P_T}\sum_{i=1}^{n} P_i\tau_i \quad \text{and} \quad P_T = \sum_{i=1}^{n} P_i \quad (11)$$

τ_{rms} root mean square delay spread.
τ_0 mean delay.

The table 4 shows the values obtained for a set of areas corresponding to the competition context.
The bandwidth needed for the video transmission is wider than the values of Bc shown in table 4. A frequency selective behavior of the channel must be expected.

Model	Area	Bc
GSM 12 rays	Urban Area	25 034 Hz
GSM 6 rays	Urban Area	23 034 Hz
UMTS 6 rays Channel A	Macro cell Low delay spread	67 600 Hz
UMTS 6 rays Channel B	Macro cell High delay spread	6 230 Hz

Table 4 Coherence Bandwidth for different standard mobile channel models

Figure 7.a shows the channel model for a 110 Hz maximum Doppler. Figures 7.b and 7.c show a realization of the channel respectively at a given instant and for a given frequency.
For video transmission, it is reasonable to envisage an occupied bandwidth between 2Mz an 70Mhz, depending on the transmission technique. In that case, figure 7.b confirms the frequency selective behavior of the channel. The emitted video signal undergoes several deep fades up to 20 dB.

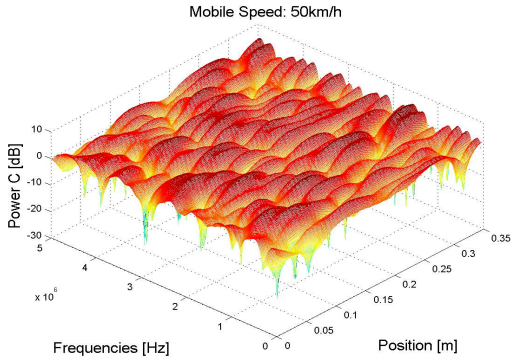

Figure 7.a 12 rays GSM channel model for urban area

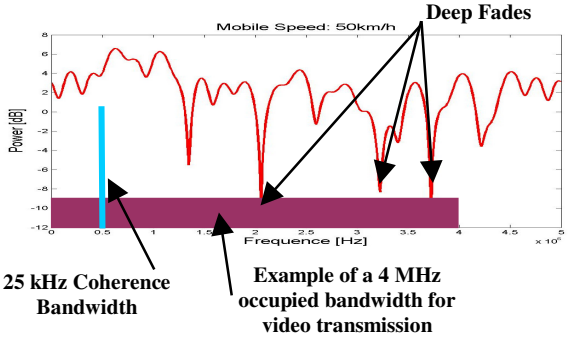

Figures 7.b Frequency domain

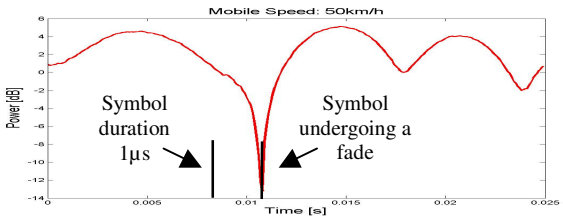

Figures 7.c Time domain

Figure 7.c shows that deep fades are also experienced in the time domain and that groups of symbols can be totally lost. Thus, fade mitigation techniques like time diversity must implemented in order to use the information given by the different delayed signals, figure 7.d. (e.g Rake Receiver).

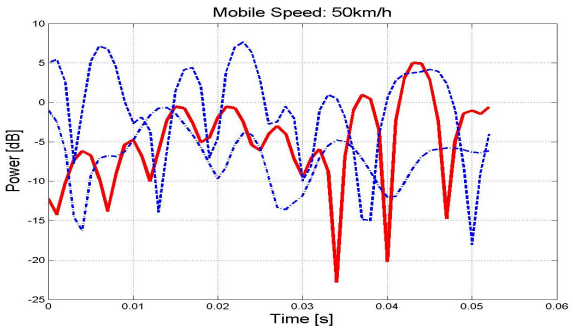

Figure 7.d Multiple superimposed delayed signals

3.3.4. Validity the power delay profiles

The simulation campaigns use standard power delay profiles for semi urban areas taken from studies made for the GSM and the UMTS standards. Concerning the speed of the mobile, these models are made for a 250 $Km.h^{-1}$ maximum mobile speed. Consequently, these profiles are suited to the micro UAV speed of 50 $Km.h^{-1}$. Nevertheless, these profiles must be taken cautiously. The GSM and UMTS standards use a lower frequency band, respectively 900-1800 MHZ and 1920-2170 Mhz and they provide a lower bit rate than the transmission payload of the micro UAV. The UMTS profiles are the most representative and they give a good idea of the length of impulse response of the transmission channel, around 5 µs, for a first modelisation of the system under Simulink. To be more precise further measures should be done under field conditions at 2.4 GHz.

3.3.5. Classification of the channel

The developments made previously allow to classify the propagation channel as slow fading – frequency selective. [Figure 8]

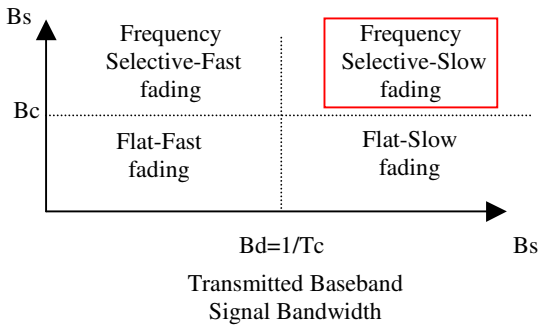

Figure 8. Matrix illustration of the different types of fading

3.4. Link Budget

The following table synthesizes the link budget. It assumes a QPSK mapping, the use of training sequences occupying 1/6 of the time slots, and the channel coding described in 4.

Required Eb/N0 (See 4.8)	3.5
T0 ambiant temperature	300K
Te receiver equivalent noise temperature	457K
Ge emitter gain	0dB
Gr receiver gain	12dB
Fp	2.4Ghz
D emitter-receiver distance	1Km
Rs symbol rate	1.02 Msb/s
Pr min = Rs.k.No(Te+T0).(Eb/N0)	-102 dBm
For a LOS transmission Pe = Pr.(1/Ge).(1/Gr).($(4.\pi.D)/\lambda)^2$	-13.95dBm
For a Non LOS transmission (Rayleigh fading). Pe ~ Pr.(1/Ge).(1/Gr).$(D)^4$	6 dBm 4 mW
For a Non LOS transmission (Rayleigh fading) plus 5 to 20dB of shadowing.	11 to 26dBm

It appears that the required power must considerably increased in the case of a Non LOS transmission, and even more for when shadowing occurs.

A solution could be to use a variable gain in the emitter to increase the power in the case of a strongly attenuated transmission.

4. Channel coding strategy

Channel coding stages are composed of a cyclic (204/188) Reed Solomon coder followed by an first (outer) interleaver, a [171,133] convolutional coder of constraint length 7 and rate ½, and a second (inner interleaver).

4.2. Inner interleaving.

In a multipath fading environment errors occurs by burst. Block codes and convolutional codes are effective over memoryless channels where errors are random. Using an interleaver the channel can be made memoryless and FEC schemes can be used.

4.3. Convolutive coding.

Convolutive codes are used for their good errors correcting properties.
The generator matrices of convolutive codes must be non catastrophic because these matrices can generate an infinite number of errors. A polynomial generator matrix G(x) is non catastrophic if and only if $\Delta_k(x)=x^S$, $S\geq 0$, where $\Delta_k(x)$ is the greatest common divisor of all determinants of all kxk submatrices of G(x), and where k is the number of inputs of the encoder. [Bos, 99]

4.4. Puncturing

A punctured convolutional code is one in which some bits are discarded at the transmitter to reduce the amount of data to be transmitted. Convolutive punctured codes allow a dynamic adaptation of the bit rate.

4.5. Interleaving

The interleaver reduces the size of large bursts of errors by spreading them. It must be chosen long enough to spread large bursts of errors occurring, for example, during deep fades due to shadowing.

4.6. RS coding.

The (204/188) RS code corrects the residual bursts of errors. The RS symbols are composed

of 8 bits. A (204,188) RS code corrects t=(204-188+1)/2=16 symbol errors. The target BER after the RS decoder is 10^{-7} which means that the BER after the convolutive coder must be 10^{-3} maximum.

4.7. Channel coding characterization

[IEEE 802.16] gave the performance of concatenated (204/188) RS and rate ½ convolutionnal coding with interleaving. A 10^{-7} BER can be achived with a 3.5 dB Eb/N0 before the decoding stages.

5. QPSK - equalization scheme

5.1 Baseband general model

The channel coding stage has just been depicted. The coded data are then transmitted alternatively with a training PN sequence. The training sequence occupies 1/6 of the time slots and is used for the channel estimation in the equalizer.

Equalization is a technique used to overcome the effects of inter symbol interference (ISI) resulting from time dispersion in the channel. The equalizer attempts to correct for the amplitude and phase distortions that occur in the channel. These distortions change with time, because the channel response is time varying. The equalizer must therefore adapt to, or track, the changing channel response to eliminate the ISI.

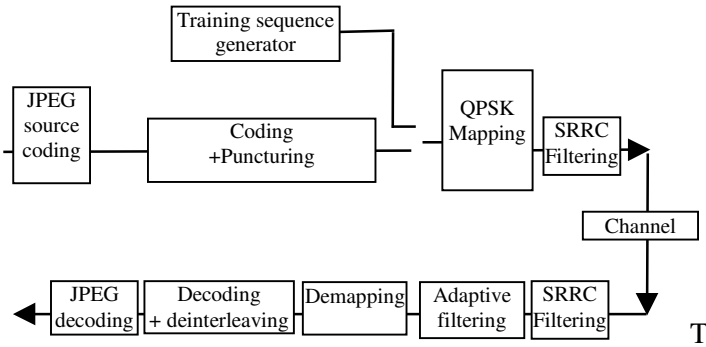

Figure 9. Architecture of the simulation.

Pulse shaping is done by a Square Root Raised Cosine filter. The Impulse Response of a Raised Cosine filter is zero at each adjacent symbol period. The Raised Cosine filter satisfies the Nyquist's criterion and is widely used, in digital communications, to limit ISI. The Square Root Raised Cosine filter allows to split this filter between the transmitter and the receiver. The RC filter has also the property to reduce the occupied transmission bandwidth B. B=Rs.(1+α) where Rs is the QPSK symbol rate. The Roll Off factor α can be adjusted to meet the bandwidth requirements. 0 <= α <=1.

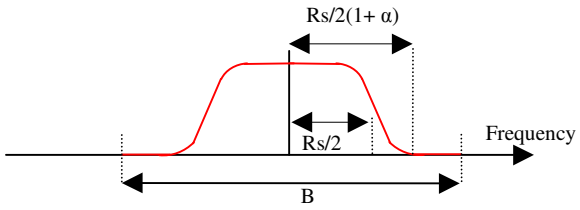

Figure 10. Raised Cosine Filter

5.2. Equalization strategies

5.2.1. LMS algorithm

The aim is to minimize the quadratic error e(n) between the filtered signal y(n) and a local replica of the signal d(n). For that, a training mode is required where a known training sequence is sent and where the weights of the filter are updated. This results in a lower operational bit rate. [eq 12]

$$y(n) = W^T(n-1).U(n)$$
$$e(n) = d(n) - y(n) \qquad \text{(eq 12)}$$
$$W(n) = W(n-1) + \mu e(n).U^*(n)$$

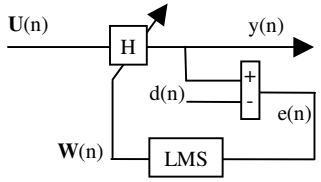

Figure 11. LMS equalizer structure

This techniques can't be used in our application since the impulse response of the channel is larger than the duration of one symbole.

5.2.1. MLSE using the Viterbi algorithm

The Maximum Likelihood Sequence Estimation using the Viterbi algorithm is the

most efficient scheme but also the most complex to implement. The complexity of the Viterbi algorithm has the form M^k, where M is the size of the constellation and k the size the size of the impulse response of the channel. For a QPSK modulation (M = 4) and a 5 symbols long IR, we need a 1024 states Viterbi decoder. The complexity can increase dramatically. An adaptive receive filter may be used prior to Viterbi detection to limit the time spread of the channel as well as to track slow time variation in the channel characteristics.

This decoder is often used for M=2 and k lower or equal to 10 [Elec, 02].

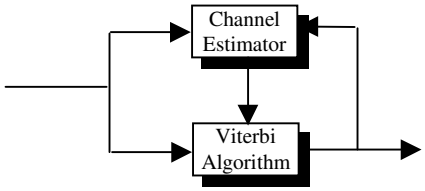

Figure 12. General form of adaptive MLSE receiver with finite-length Desired Impulse Response.

5.2. Trade off between the bit rate and the complexity of the adaptive filter.

Assuming a 5µs long mobile channel impulse response (12 rays model for UMTS), if the adaptive filter allows to correct ISI over 5 symbols, then the minimum symbols duration is 5/5 µs. Assuming a QPSK mapping, a RS 204/188 code followed by a rate 4/3 convolutive-punctured code, and taking into account the insertion of a training sequence occupying 1/6 of the data, then the video bit rate is approximately 1.15Mbits.s^{-1}. This corresponds to a transmission bandwidth of 2.30 MHz. Therefore, the system can provide the required 1.12Mbits.s^{-1} video bit rate but can't allow any evolution of the system as the use a higher coding rate or of longer training sequences.

If the bit rate increases techniques allowing the transmission of higher data rates must be considered.

6. OFDM transmission scheme

6.1 OFDM Theory

Orthogonal Frequency Division Multiplexing allows to increase the duration of each symbol while keeping the same bit rate, by multiplexing the symbols on several carriers. [EN 700 144], [802.11a]. This technique transforms a frequency selective wide band channel into a group of narrow band non selective channels, which make it robust against large delay spreads, by preserving orthogonality in the time domain. Moreover, the introduction of cyclic redundancy at the transmitter reduces the complexity to only FFT processing at the receiver, [Fig. 11].

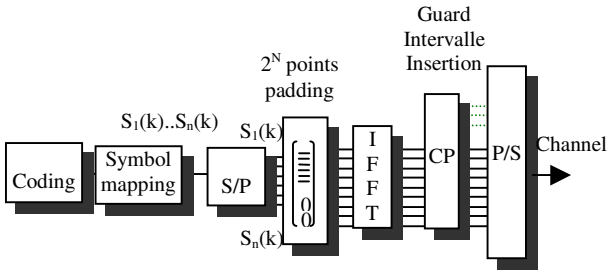

Figure 13. . OFDM Modulator

The channel variations over an OFDM symbol block destroys the orthogonality between the subcarriers resulting into inter-carriers interference (ICI) which can be mitigated by a frequency domain equalizer (FDE) block after the FFT operation, [Fig. 12].

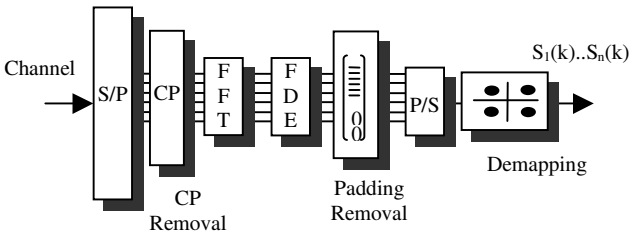

Figure 14. OFDM Demodulator

A known training sequence of symbols (i.e a PN sequence) is sent alternatively with the data symbols over the channel in order to update the coefficients of the FDE, which results in a lower operational data rate, [Fig. 13].

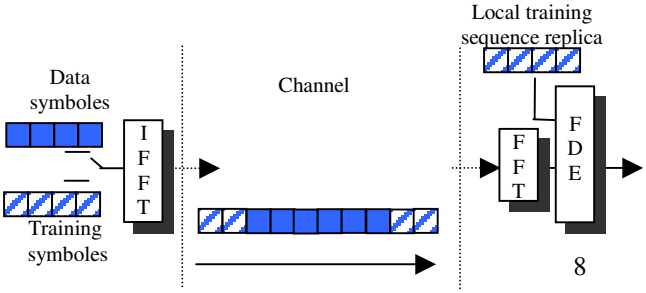

Figure 15. Training sequence

The OFDM has also the advantage of having good spectral efficiency properties; however, it has several weaknesses.

It doesn't capitalize on channel diversity. Moreover, due to frequency flat fading, the transmitted information on one OFDM subchannel can be irremediably lost if a deep fade occurs. OFDM is particularly sensible to bursts of errors making the use channel coding mandatory, i.e a RS code associated with interleaving and convolutive coding. Finally, the fact that the OFDM uses several carriers makes it sensible to non linearities in the amplifiers which requires an important back-off by as much as 10 dB.

6.2. Length of the cyclic prefix (CP)

The length of the cyclic prefix is chosen lower or equal to a quarter of the OFDM symbol duration, and it must be greater or equal to the channel impulse response. A 5*µs CP has been added [fig. 14]

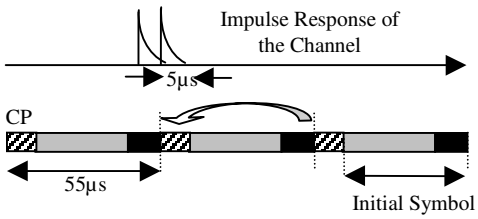

Figure 16. Effects of the cyclic prefix against ISI

6.3. Architecture of the transmitted frames

The OFDM scheme allows to transmit higher data rates than a simple QPSK scheme.
The initial goal was to provide either 14 i/s at a low resolution [table1 B] or 3.3 i/s in a high resolution [table1 D], that is a 3.5 Mbps.s^{-1} bit rate. Assuming a QPSK mapping, a RS 204/188 code followed by a rate 4/3 convolutive code, training symbols occupying 1/6 of the OFDM symbols, then the symbol rate is approximately 3.0383 Msymbols/s.
As a rule of thumb, if the RMS delay spread of the channel is lower than Tsymb/10, then channel is not frequency selective [Cos, 2001].

Tsymb is the OFDM symbol duration. Therefore, for 5µs Trms, the symbol duration must be at least 50 µs (55 µs when the cyclic prefix is considered) which corresponds to a 20Ksymps carrier frequency.
Consequently, the number of needed carriers is $3.083.10^{6}$x55.10^{-6} = 170. The DC component must be added which is not used. We get 171 carriers. Therefore, a 256 points IFFT will be used. The unused frequencies are zero padded, some of them (8 as in the 802.16a standard) can be used as pilot frequencies to give another way to estimate the channel. It corresponds to an occupied bandwidth of $257/(55.10^{-6})$ = 4.68 MHz. [fig 13].

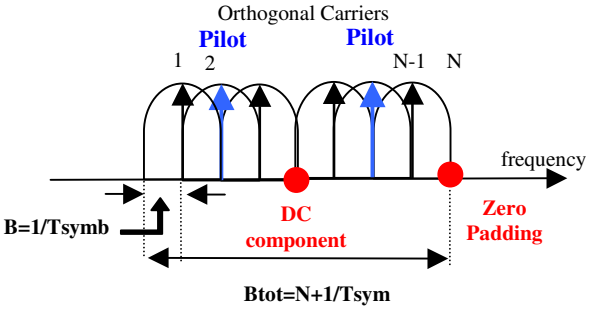

Figure 17. OFDM carriers

6.4. Proposed architecture

The table 5 sums the choices made to provide either 14 i/s at a medium resolution [table1 B] or 10 i/s at a high resolution [table1 D].

RS code rate	204/188
Convolutive code rate	4/3
Puncturing rate	6/4
Training sequence type	PN sequence
data/training symbols alternance	20 data symbols followed by 4 training symbols
QPSK Symbol rate after coding	3.083 Msymb.s^{-1}
OFDM symbol duration	50 µs
Number of data carriers	170
Number of pilot carriers	8
Total number of carriers	256
Length of the CP	5 µs
Occupied Bandwidth	4.68 MHz

Table 5. Proposed architecture

The figure bellow shows the number of data carriers required versus the video bit rate. The horizontal lines represents 64, 128 and 256 carriers. A 1.2 Mbits video bit rate can be transmitted with 50 carriers, and therefore by using a 64 points IFFT.

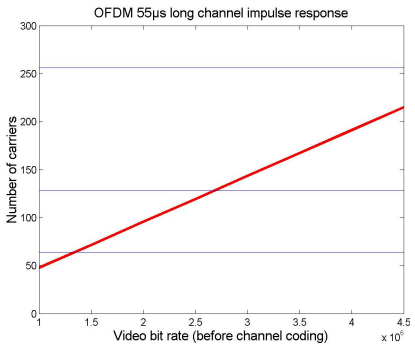

Figure 18. Number of data carriers VS the video bit rate.

7. Direct sequence spread spectrum transmission scheme

7.1. CDMA theory

7.1.1 Spreading and Scrambling

Spreading is done by multiplying the data with a spreading code, the resulting signal is a bit stream with a much higher data rate, depending on the current spreading factor. At the receiver, the spread signal is multiplied by a local in phase replica of the spreading code. The resulting chips are then accumulated to form symbols. By spreading the spectrum of the signal over a much larger bandwidth one gains immunity against noise and path distortions [fig. 14].

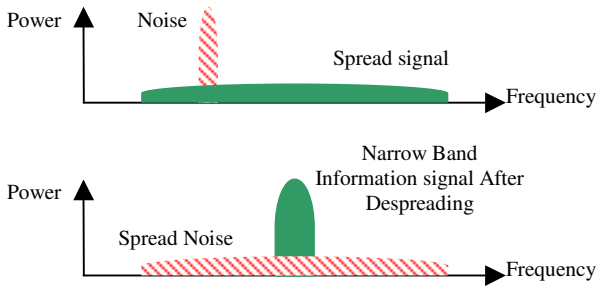

Figure 19. Illustration of the immunity against noise.

The data are spread with orthogonal spreading codes [Table 6]. Orthogonal codes have zero cross-correlation. These codes allow different data channel to use the same frequency band. The major problem with spread spectrum is that data rates higher than about 10Mbps are difficult to achieve due to the large bandwidth and processing needed. A solution to reduce the bandwidth could be to split the data stream between several channels by using orthogonal codes. In this case, several rake receivers should be used (see 6.1.3.) resulting in a higher complexity.

	(1,1,1,1)	(1,1,-1,-1)	(1,-1,1,-1)	(1,-1,-1,1)
(1,1,1,1)	4	0	0	0
(1,1,-1,-1)	0	4	0	0
(1,-1,1,-1)	0	0	4	0
(1,-1,-1,1)	0	0	0	4

Table 6. Example of CDMA orthogonal codes

It may seem to be attractive to replace PN codes which have non-zero cross-correlations but things are not going perfect. The cross-correlation value is zero only when there is no offset between the codes. In fact, they have large cross-correlation values with different offsets, much larger than PN codes. The autocorrelation property is usually not good either. Orthogonal codes have an application in perfectly synchronized environments.

Scrambling the spread signal with a PN sequence usually allows to use the same spreading pattern between adjoining cells. But also, if the maximum delay spread of the path is greater than a bit period, the receiver has a better chance of determining bit synchronization by using the spreading and scrambling codes together [TI, 00]. OVSF (Walsh-Hadamard) codes has been used for the spreading.

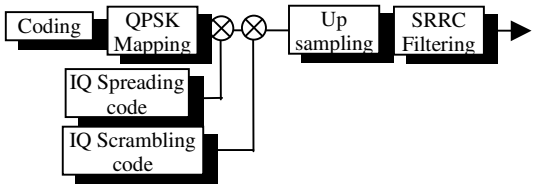

Figure 20. Spread spectrum emitter

7.1.2. Architecture of the data and pilot channels

The information data stream is transmitted over one or several channels. The data are contained into frames. Each frame is divided into slots. The beginning of each slot contains a training sequence which can be used for channel estimation.
An extra channel is used for the pilot transmission, with a higher power than the data channels. The pilot channel contains a training sequence of lower bit rate than the data but its

spreading factor is higher than the data channels. This result in the same chip rate for both the data channels and the pilot channel.

7.1.3. Rake receiver

The received signal can be written as:

$$y(t) = \sum_{j=0}^{J-1} c_j . u(t - dj) + g(t) \quad \text{(eq. 13)}$$

u is the transmitted signal. The channel is modeled as a tap filter with complex coefficients c_j and delays d_j. g(t) is the AWGN

The Rake receiver uses time diversity to mitigate the multipath-induced fading that results from users' mobility. The strongest multipath components have a dedicated Rake finger device. Each finger follows the same step, namely:

1. Descrambling and despreading
2. Integration and dump
3. Combining of the symbols received by each finger according to a a combining scheme like Maximum Ration Combining MRC.
4. The combined output are transferred to a decision device to decide on the transmitted bits.

A channel estimation is performed on each finger to correct the phase and the amplitude. The advantage of using a pilot channel dedicated to channel estimation instead of the training symbols inserted in the data slots is that more symbols are available. This is why we have chosen to use the pilot channel for the simulation.

The path search has not been developed for this simulation, it will be further described in another study. For the moment, the knowledge of the delays specified in the channel model is used instead of the path search.

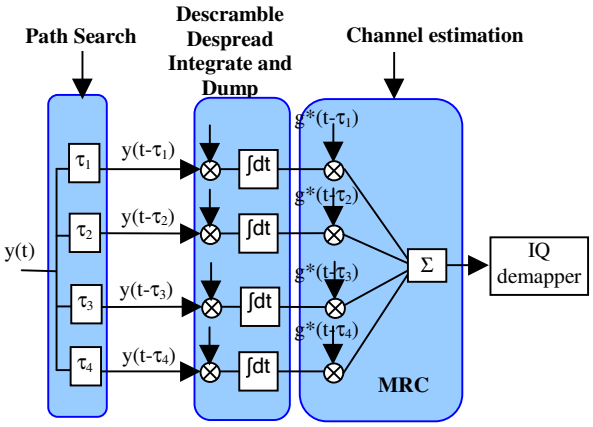

Figure 21. The four fingers rake receiver used for the simulation.

A cdma system can distinguish (Tmax-Tmin)*W+1 paths, provided that the spacing between two paths is at least of one chip. Tmax is the delay of the last path and Tmin the delay of the first path, W is the bandwidth of the spread signal. W=1/Tc

A search strategy is to search paths at a ½ chip period, by successive correlations of the signal with a local sequence associating the spreading code and the scrambling code. When this rough search is finished further correlations are done at the oversampling rate (1/8 of the chip period) to find the eye maximum. Finally only the main paths are kept (4 in the simulation).

7.2. Proposed architecture

The table 7 sums the choices made to provide either 14 i/s in a low resolution [table1 A] or 3.3 i/s in a high resolution [table1 D].

Architecture 1
Video 1.12 Mbits/s
Coding: RS (204/188) + interleaving+ 4/3 Convolutionnal punctured code + Mapping QPSK
1 data channel, 1pilot channel
QPSK Symbol Rate: 0.8102 Msymb/s
Spreading: length 64 OVSF code
Scrambling: PN code
Chip rate on channel I and channel Q: Fc = 1.6204x64 = 51.8536 Mchips/s
Pilot bit rate on channel I and channel Q: Fc/256 = 202.6 Ksymb/s
Spreading : length 256 OVSF code
Scrambling : PN code
SRRC roll off 0.4
Bandwidth = RS.(1+α) = 51.8536 x (1+0.4)= 72.6 MHz
One rake receiver

Table 7. Proposed architecture for a 1.12 Mbits/s video stream

The table 8 sums the choices made to provide either 14 i/s in a medium resolution [table1 C] or 10.3 i/s in a high resolution [table1 D]. The combining of two rake receivers is proposed to reduce the bit rate per data channel. Each data channel would use an orthogonal OVSF code. But further studies must be done to evaluate the complexity of such a system.

Architecture 1
Video 3.5 Mbits/s
Coding: RS (204/188) + interleaving+ 4/3 Convolutionnal punctured code + Mapping QPSK
2 data channel, 1pilot channel
QPSK Symbol Rate: 2.5319 Msymb/s
Spreading: length 32 OVSF code
Scrambling: PN code
Chip rate on channel I and channel Q: Fc = 1.6204x64 = 40.5 Mchips/s
Pilot bit rate on channel I and channel Q: Fc/256 = 316.5 Ksymb/s
Spreading : length 256 OVSF code
Scrambling : PN code
SRRC roll off 0.6
Bandwidth = RS.(1+α) = 40.5 x (1+0.6)= 64.9 MHz
2 rake receivers

Table 8. Proposed architecture for a 3.5 Mbits/s video stream.

8. Conclusion

The OFDM and the CDMA-Rake transmission schemes have been preferred to the QPSK associated with equalization scheme. They allows the transmission of higher data rates and they will be more flexible to evoluate in the futur.

Both the technical aspects of these transmission schemes and the channel model must be studied more deeply.

This study has been a first approach toward technical solutions to the multipath issue. It open several research fields for the future at SUPAERO.

[Bos, 99] Channel Coding for Telecommunication. Martin Bossert, 1999, Wiley

[Bur, 03] Charge Utile d'Observation pour Micro Drone à base d'une Micro Caméra Numérique. Philipe Burdinat, 2003, CIMI – SUPAERO

[Cos, 2001] Orthogonal Frequency Division Multiplexing (OFDM): Tutorial and Analysis. Erich Cosby. ECE 5664 Project, 2001

[Elec,02] Radiocommunications Numériques /1 Collection EEA, 2002, DUNOD

[IEEE 802.16] FEC Performance of Concatenated Reed Solomon and Convolutional coding with Interleaving. IEEE 802.16 Working Group, 2000.

[Fran, 97] Analyse d'un Schéma de Transmission pour Communications Mobiles par Satellites, Michel-Guy Françon 1997, Thèse ENSAE

[Jakes, 94] Microwave Mobile Communications, IEEE press,1994.

[Ngoc, 94] Coded Modulation Techniques for Fading Channels, S.Hamidreza Jamali & Tho Le Ngoc 1994, Kluwer Academic Publishers

[Saunders, 99] Antennas and Propagation for Wireless Communication Systems, Simon & Sanders 1999, Wiley

[TI, 00] Implementation of a WCDMA Rake Receiver on a TMS320C62X DSP Device. Texas Instruments, Application Report, July 2000.

[Cos, 2001] Orthogonal Frequency Division Multiplexing (OFDM): Tutorial and Analysis. Erich Cosby. ECE 5664 Project, 2001

[DVB] Digital Video Broadcasting developed from the ETSI EN 300 744 standard.

[802.11a] IEEE standard for Wireless Lans http://grouper.ieee.org/groups/802/11

[802.16] Comparison of QPSK/QAM OFDM and Spread Spectrum for the 2-11 GHz PMP
BWAS. M.Sellars & D.Kostas, IEEE 2000